IEEE Access
Multidisciplinary ⋮ Rapid Review ⋮ Open Access Journal

Received 28 March 2024, accepted 23 May 2024, date of publication 3 June 2024, date of current version 12 June 2024.

Digital Object Identifier 10.1109/ACCESS.2024.3408412

RESEARCH ARTICLE

Accurate Reconstruction of the 12-Lead Electrocardiogram From a 3-Lead Electrocardiogram Measured by a Mobile Device

MARJAN N. MILETIĆ[1,2], VLADIMIR A. ATANASOSKI[1,2], PETRA P. BELIČEV[1,2], GORAN M. GLIGORIĆ[1,2], UROŠ M. RALEVIĆ[2,3], JELENA B. KRŠIĆ[1,2], ALEKSA D. OBRADOVIĆ[4], ALEKSANDAR LAZOVIĆ[1], DANKA B. STOJANOVIĆ[1,2], JOVANA PETROVIĆ[1,2], (Member, IEEE), RADE BABIĆ[5], DEJAN VUKAJLOVIĆ[4], LJUPČO R. HADŽIEVSKI[1,2], BOŠKO P. BOJOVIĆ[1,2], DORIN PANESCU[6], (Fellow, IEEE), AND BRANISLAV VAJDIĆ[2]

[1]Department of Atomics Physics, Vinča Institute of Nuclear Sciences–National Institute of the Republic of Serbia, University of Belgrade, 11000 Belgrade, Serbia
[2]HeartBeam Inc., Santa Clara, CA 95050, USA
[3]Centre for Solid State Physics and New Materials, Institute of Physics–National Institute of the Republic of Serbia, University of Belgrade, 11000 Belgrade, Serbia
[4]Institute for Cardiovascular Diseases "Dedinje," 11000 Belgrade, Serbia
[5]Faculty of Medicine, University of Belgrade, 11000 Belgrade, Serbia
[6]BIOTRONIK CRC EP, Santa Clara, CA 12444, USA

Corresponding author: Marjan N. Miletić (marjanmil@vin.bg.ac.rs)

This work was supported in part by the Ministry of Science, Technological Development and Innovation of the Republic of Serbia; and in part by HeartBeam Inc., Santa Clara, CA, USA.

This work involved human subjects or animals in its research. Approval of all ethical and experimental procedures and protocols was granted by the Ethics Committee for Human Research of the Vinca Institute of Nuclear Sciences, National Institute of the Republic of Serbia, University of Belgrade, Belgrade, Serbia, under Application No. 116-1-2/2023-000.

ABSTRACT Clinical outcomes of several acute conditions, including myocardial infarction (MI), the most common cause of death, can be improved by timely diagnostics based on electrocardiography (ECG). However, current diagnostic technologies include a large number of wired ECG electrodes, which require accurate placement by trained personnel. The ideal ECG device would be suitable for self-measurement, i.e., would have a small number of electrodes, be mobile or portable, and provide an accurate diagnosis. However, these aims have not been met using the same device. A recently developed handheld ECG device with three quasi-orthogonal leads opened the door for mobile assessment of the three-dimensional cardiac vector by self-measurement. We hypothesize that the information provided is sufficient for accurate reconstruction of the 12-lead ECG. We propose a reconstruction algorithm based on the segment-by-segment 4-matrix (4M) transformation applied to the P wave, QRS complex, ST segment, and T wave. The accuracy of the 4M method was tested using data obtained from 64 healthy volunteers. The 4M method reconstructed the standard 12-lead ECG with a 0.96 mean cross-correlation for all leads and provided meaningful clinical results. A back-to-back comparative study demonstrated the superiority of the proposed method over the traditional EASI method. In addition, the results provide evidence of the capability of the 3-lead 4M technology to accurately reconstruct the full cardiac vector from a single measurement, which distinguishes it from competition. Although further clinical investigation is necessary, wireless operation and high accuracy make the proposed method potentially suitable for remote monitoring and self-assessment.

INDEX TERMS Cardiac vector, mobile ECG, 12-lead reconstruction.

I. INTRODUCTION

Cardiovascular disease is the leading cause of death worldwide, accounting for approximately 32% of the total global

The associate editor coordinating the review of this manuscript and approving it for publication was Hasan S. Mir.

deaths in 2017 [1]. Timely diagnosis and regular monitoring of a number of conditions, such as myocardial infarction (MI) and acute decompensated heart failure, have been shown to significantly reduce mortality rates [2]. Therefore, special attention is directed towards the development of reliable and economically accessible technologies and algorithms for diagnosing and monitoring cardiovascular diseases at any time or place [3], [4].

ECG is a routine diagnostic and monitoring technique that reveals many conditions, including life-threatening arrhythmias, pericarditis, ischemia, and acute MI [5]. Standard 12-lead ECG is performed by placing 10 measuring electrodes connected by wires onto a patient at rest. Its portable derivative, Holter, is routinely used for 24-h remote monitoring of patients. However, the large number of electrodes and the need for an operator for accurate placement make it inconvenient for self-application. The wired connection further complicates mobile monitoring applications because of the signal artifacts and noise caused by the wires touching the limbs. These disadvantages have prompted intense efforts towards developing wireless ECG devices, which are optimized to acquire the maximum amount of information about cardiac electrical activity from as few recording sites as possible [6]. Ideally, information regarding the dynamics of a full three-dimensional (3D) cardiac vector would be extracted [7].

Among a plethora of ECGs with a reduced number of leads [8], the EASI configuration has been the most widely studied and used. It is based on a quasi-orthogonal lead system that uses four electrodes conveniently located at anatomical positions and a ground electrode. A standard 12-lead ECG is reconstructed by applying the universal transformation matrix developed by Dower et al. [9] and commercialized by Phillips Medical Systems. It has been shown that the reconstructed ECG is comparable to the standard 12-lead ECG in the presence of various cardiac rhythm abnormalities [10], acute myocardial ischemia and past infarction [11], [12], ST deviation [13], ST-elevation due to acute MI, and acute coronary syndrome [14]. An improved EASI reconstruction with computed new transformation coefficients from a larger data set was presented by Feild et al. [15]. While greatly contributing to the reduction in the number of electrodes, the EASI device uses cable electrodes, which complicates its application at home and in emergency situations, for example, in detecting acute myocardial ischemia [16].

On the other hand, the commonly used mobile ECG devices with wireless capability, AliveCor (Kardiamobile), and Apple Watch (Apple) [17], [18], measure a single ECG lead. Although highly suitable for self-assessment, single-lead registration is not useful for diagnosing myocardial ischemia and acute coronary syndromes, including acute MI [19]. Specifically, single-lead registration is unable to reconstruct cardiac vector activities, whereas it was shown that even with the 3-lead system, it is possible to detect coronary artery occlusion using automated vectorcardiographic analysis of the ST segment [20]. A possible solution to this problem is consecutive 1-lead measurements at different positions to reproduce a 3-lead ECG [21], [22]. However, the length and complexity of the measurement procedure make it impractical in emergencies [23]. Finally, the importance of full 3D vector reconstruction has recently been confirmed by a study showing a relatively low sensitivity (65%) to the occlusive MI of a 4-lead mobile device with electrode positions restricted to the precordial area [24].

The reconstruction algorithm itself faces two important challenges: the quality of reconstruction from non-simultaneously recorded few-leads and reference ECGs, such as a recording with a newly acquired mobile device and a recent reference recording taken in a hospital, and the quality of reconstruction of all ECG signal segments by a single matrix.

In this paper, we present a novel 4-matrix (4M) method for the reconstruction of a 12-lead ECG from three quasi-orthogonal leads obtained by a single non-simultaneous ECG recording using a prototype of a wireless handheld AIMIGo (HeartBeam, Inc.) (AIMIGo). AIMIGo is an ECG credit-card-sized device already been described [20], [25]. The algorithm is based on the matrix transformation applied independently to the P wave, QRS complex, ST segment, and T wave. All transformation matrices were personalized. This method was tested in a study of 64 healthy volunteers. The study was designed to enable 4M matrix calibration, a test against the 12-lead ECG as a reference, and comparison with the EASI method. In addition, 4M is compared with the 1M method, which uses a single matrix on the entire ECG signal without segmenting it.

II. THE METHOD

The application of the 4M reconstruction method entails 3-lead ECG preprocessing for signal quality improvement and 12-lead ECG reconstruction by application of 4M matrices to the three leads. The 4M transform matrices T are defined on four featuring and diagnostically relevant segments of the heart cycle: the P-wave matrix (T_P), QRS-complex matrix (T_{QRS}), T-wave matrix (T_T), and ST-segment matrix (T_{ST}). They were set using a segment-by-segment calibration procedure performed on the measured signals. The method was tested against a standard 12-lead ECG and compared with the improved EASI reconstruction ('new limb' [15]) on a test set measured for this purpose. Here, we present the preprocessing algorithm ubiquitous to all signals and procedures, 4M calibration algorithm, 4M reconstruction procedure, calibration and test datasets, and performance metrics. All the presented algorithms were implemented in MATLAB (MathWorks Inc.).

A. PREPROCESSING

All ECG signals, both 3- and 12-lead, were sampled at 500 Hz and preprocessed using the following filters (Fig.1):

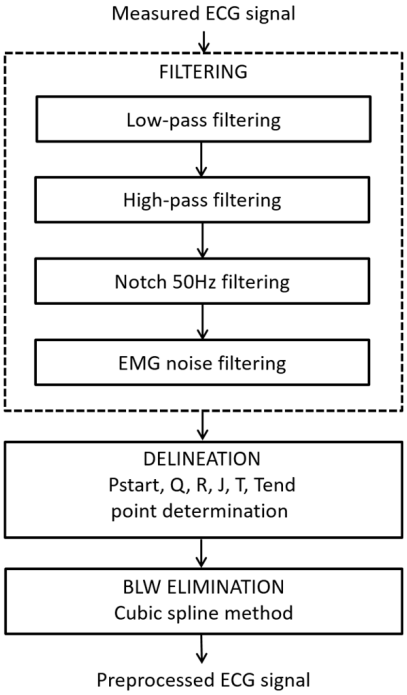

FIGURE 1. Flow chart of the preprocessing algorithm comprising filtering, delineation and BLW elimination steps.

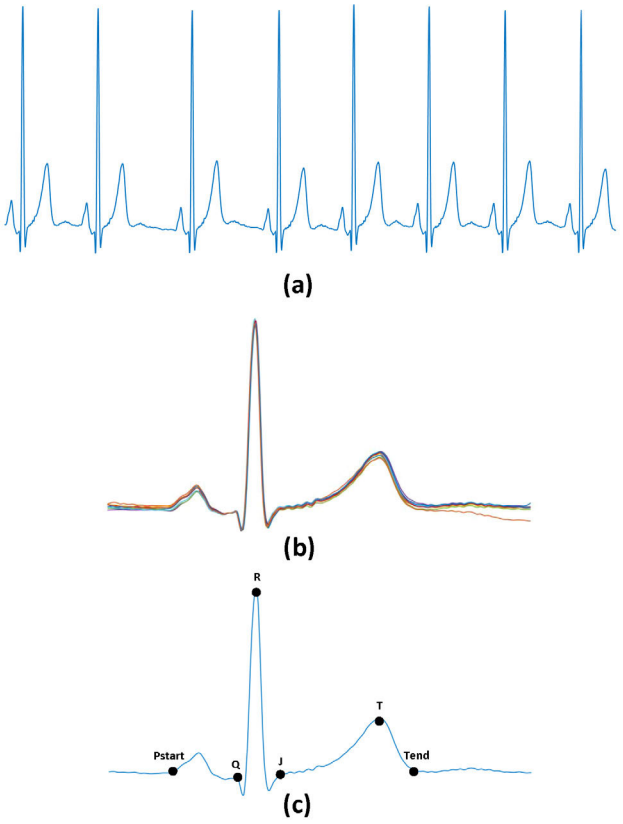

FIGURE 2. An example of median beat construction. (a) ECG signal, (b) heartbeats overlapped to match their R points, (c) median beat with marked fiducial points.

- low-pass 5th-order Butterworth filter with a cutoff frequency of 150 Hz to eliminate high-frequency noise.
- high-pass 2nd-order Butterworth filter with a cut-off frequency of 0.05 Hz to eliminate small BLW,
- 2nd-order IIR notch filter with the frequency of 50Hz in both forward and reverse directions for removal of power-line interference,
- morphology-preserving algorithm to eliminate electromyographic noise [26].

After filtering, all signals were delineated using a proprietary automated delineation algorithm to determine the Pstart, Q, R, J, T, and Tend points, which correspond to the start of the P wave, maximum amplitude of the Q wave, maximum of the QRS complex, J point, maximum amplitude of the T wave, and the end of the T-wave, respectively. Finally, the baseline wander was eliminated using a cubic spline through points determined in relation to the Q points.

B. 4M CALIBRATION

Calibration was performed on the median beats, each representing one lead (Fig. 2). To obtain the median, a- lead is divided into heartbeats defined on the interval [R - 0.45 RRmed, R + 0.55 RRmed], where RRmed is the median of the RR intervals of all heartbeats in that lead. Prior to the calculation of the median beat, all heartbeats were aligned to match their R-points, as shown in Fig. 2b. The median beat was calculated by finding the median of all heartbeats at each sample point, as shown in Fig. 3b. The median beats of the 3- and 12-lead ECG signals were resampled to longer beats. Resampling was performed on the [J, T] and [T, Tend] segments in Fourier space.

The coefficients of the transformation matrices T_P, T_{QRS}, and T_T were calculated between the corresponding segments of the median beats of the 3-lead and 12-lead ECG calibration signals using the least-squares method (Fig. 3). The segments are defined as

- P calibration segment – [Pstart – 20 ms, PQmin + 20 ms]
- QRS calibration segment – [PQmin – 20 ms, J + 20 ms]
- T calibration segment – [J - 20 ms, Tend],

where the PQmin reference point is calculated as the point in the interval [Q–60 ms, Q – 20 ms] from which the sum of the heart-vector magnitudes in this interval is minimal. Here, the heart-vector magnitude is defined as the root sum of the squares of all three leads at a certain time point. The overlapping of the segments helps to smooth the discontinuities between segments in the reconstruction process, as described in the following section.

For the same reason, the nearly isoelectric signal over the entire ST segment makes the reconstruction of this segment particularly challenging. Owing to the near-zero amplitudes in a healthy population, regression yields a large uncertainty in the T_{ST} matrix elements, causing noise in the reconstructed signal. To avoid this problem, the T_{ST} is calculated as a linear

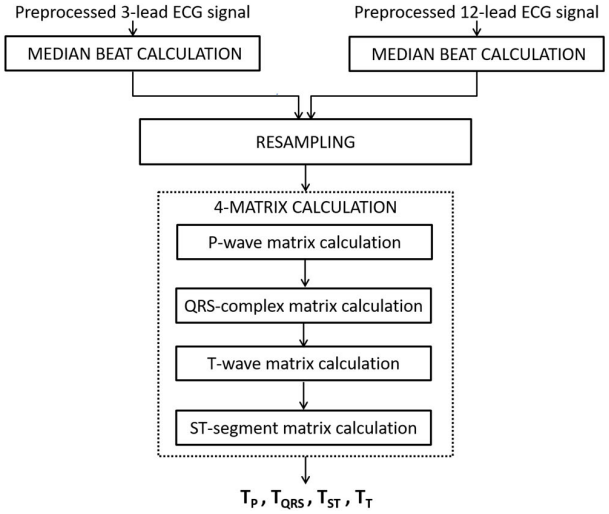

FIGURE 3. Flow chart of 4M calibration algorithm.

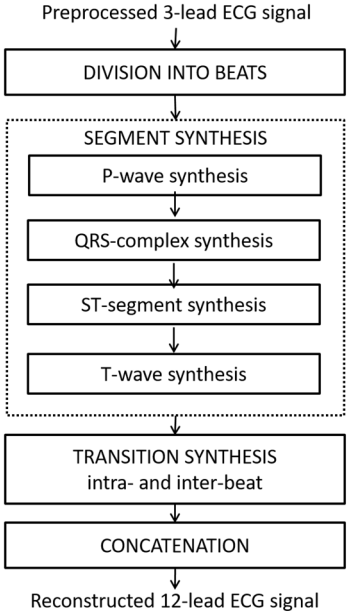

FIGURE 4. Flow chart of 12-lead synthesis algorithm using 4-matrices.

combination of T_{QRS} and T_T:

$$T_{ST} = T_{QRS} + \frac{P_T}{P_T + P_{QRS}}(T_T - T_{QRS}) \quad (1)$$

with weighting coefficients proportional to the sum of the heart vector magnitude on these segments, P_T and P_{QRS} (see the Appendix for the mathematical formulation).

C. 12-LEAD ECG RECONSTRUCTION

The 12-lead ECG reconstruction begins with 3-lead ECG signal preprocessing described in Section II-A. The processed 3-lead signal is divided into beats, with the i^{th} beat defined on the interval [$Pstart_i$-40ms, $Pstart_{i+1}$-40ms] (Fig. 4). The four segments of the i^{th} beat are defined as:

- P segment – [$Pstart_i$ – 40 ms, $PQmin_i$],
- QRS segment – [$PQmin_i$, J_i],
- ST segment – [J_i, J + 80ms],
- T segment – [J_i + 80 ms, $Pstart_{i+1}$ - 40ms],

and is multiplied by the corresponding four matrices. The intervals between the segments of a beat (intra-beat transition segments) and segments between beats (inter-beat transition segments) were reconstructed using transient matrices. The elements of a transient segment matrix change linearly from those of the previous segment matrix to those of the following segment matrix. For example, the transient matrix applied between the P and QRS segments was constructed by linear interpolation of the T_P and T_{QRS}. The elements of the inter-beat matrices linearly connect the T_T of one beat to the T_P of the following beat.

The matrices were used for the reconstruction of the measured leads (I, II, V1-V6) and count 4 × 8 elements. Leads III, aVR, aVL, and aVF are derived from leads I and II, as in the standard ECG device.

The 4M reconstruction was compared with the single-matrix reconstruction. It is applied to the same 3-lead ECG recordings as the 4M reconstruction and consists of simple multiplication of the whole signal by a calibration matrix (3-lead 1M (3L1M) method). The matrix was calibrated using the median beat as described in the previous section. 1M does not require signal segmentation, and in that sense, it is similar to the EASI reconstruction.

D. DATA SET

The method was validated on a dataset measured on 64 healthy volunteers using a 3-lead mobile and standard ECG device. The volunteer set consisted of 33 females and 31 males with an average age of 38.6 ± 11.0 and a body-mass index of 25.8 ± 4.0.

The 12-lead ECG and corresponding EASI configuration measurements were performed using an EDAN SE-1515 PC 18-lead ECG device (EDAN Inc., Shenzhen, P. R. China) with a sampling frequency of 500 Hz. This device measures 12 standard leads and six additional precordial leads. The EASI configuration was realized by placing three additional precordial electrodes at positions E (at the level of the fifth rib on the lower sternum), I (in the right midaxillary lines at the same level as E), S (on the manubrium sterni), and A (in the left midaxillary line at the same level as E). Electrode position A corresponds to the position of the precordial electrode V6, and the ground electrode position (the ankle joint of the right leg) corresponds to the ground electrode of the standard 12-lead ECG (Fig. 5a and 5b).

The 3-lead ECG measurements were performed using AIMIGo, a mobile 3-lead credit-card-sized device with the acquisition software running on an Android smartphone [27]. The position of AIMIGo is on the left side of the chest (above the heart), close to the sternum, and approximately 3-5 cm below the clavicle (Fig. 5c and 5d). The device uses two finger and two chest electrodes with a resistive network to

measure three quasi-orthogonal leads: a lateral lead (equivalent to standard lead I), a vertical lead (similar to standard lead V3), and a sagittal lead (similar to standard lead aVF) [20], [28].

The measurement protocol was designed to test the matrix calibration on non-simultaneously recorded standard and 3-lead ECGs, as this best mimics the real-world calibration of the mobile ECG device. It consisted of recording 5 non-simultaneous 30-second ECG signals in the following order:

a) AIMIGo 3-lead mobile ECG calibration signal,
b) 12-lead standard ECG calibration signal,
c) EASI 3-lead ECG diagnostic signal,
d) AIMIGo 3-lead ECG test signal – same as a),
e) 12-lead ECG reference signal – same as b),

with a 5-minute break between the recordings.

All measurements using the mobile device were performed in a semi-reclined sitting position (at approximately 45-degree incline to the vertical), and all measurements using the standard device were in the supine position. The recordings affected by large baseline wonder, electromyographic noise, and motion artifacts were repeated until a satisfactory quality was ascertained by visual inspection.

The total number of recordings in the set was 320:128 from the calibration set (a and b) and 192 from the test set (c, d, and e).

This study was approved by the Ethics Committee for Human Research of the Vinca Institute of Nuclear Sciences, National Institute of the Republic of Serbia, University of Belgrade, Belgrade, Serbia (no. 116-1-2/2023-000). All the study participants signed a written consent form.

E. CLINICAL VALIDATION

Clinical validation of the 3-lead 4M method was performed by two expert cardiologists (R.B. and D.V.), who independently compared the anonymized 12-lead signals reconstructed by 4M against the reference ECG. They marked one of the following three possible outputs:

1. Adequate matching - negligible differences in signal shapes or voltages;

2. Acceptable matching: visible differences in signal shapes or voltages, but these differences do not affect the appropriate clinical decision on further diagnostic or therapeutic procedures.

3. Inadequate matching - there are significant differences in signal shapes or voltages that affect the appropriate clinical decision.

The observed diagnostically relevant features followed current recommendations and guidelines [29], [30], [31], [32], [33].

F. PERFORMANCE METRICS

To assess the diagnostic potential of the 3-lead ECG device and compare it to the EASI the method, we evaluated the reconstruction of both the signal morphology and cardiac axis angle. Morphology was assessed directly from the ECG time series. The cardiac axis angle at a certain point in time is calculated as the angle between the cardiac vector projection onto the frontal plane and has values in the range of -180° to 180°.

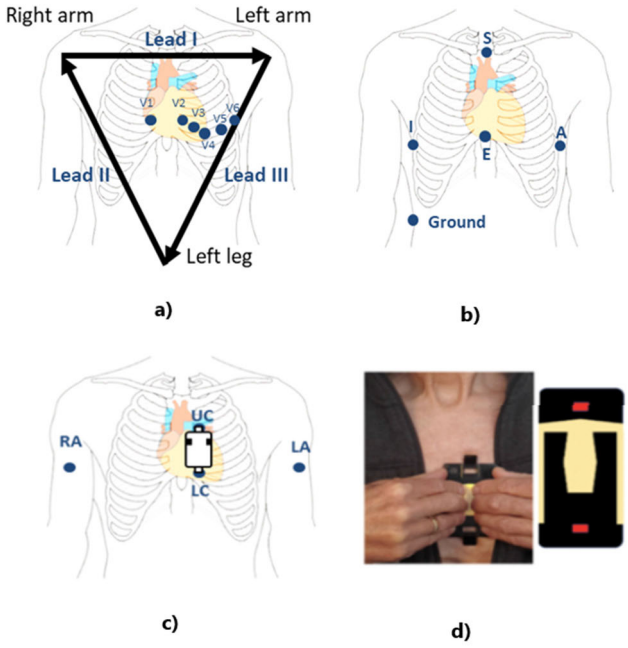

FIGURE 5. a) Position of electrodes in a) standard 12-lead ECG, b) EASI and c) AIMIGo measurements. d) Application of AIMIgo 3-lead ECG device [27].

The reconstruction metrics use a generic cross-correlation (CC) function given as

$$CC\,(A,B) = \frac{1}{N-1}\sum_{i=1}^{N}\left(\frac{A_i-\mu_A}{\sigma_A}\right) * \left(\frac{B_i-\mu_B}{\sigma_B}\right) \quad (2)$$

where A/B is the reconstructed/reference ECG signal, $\mu_{A/B}$ and $\sigma_{A/B}$ the corresponding mean and standard deviation, respectively, and N is the total number of samples of the median beat.

Morphology was first assessed lead-by-lead by applying (2) to median heartbeats. This yields the cross-correlation amplitude metric XCORR for each lead (I, II, III, aVR, aVL, aVF, V1–V6) as well as the mean XCORR as a global metric on the set. Because the cardiac axis angle calculation requires multiple leads, this metric is not applicable.

The reconstruction of the diagnostically relevant morphological features on each median-beat segment, namely the P-, R-, and T-wave amplitudes and the mean amplitude of the ST segment (V_P, V_R, V_T, and V_{ST}), was evaluated using their Pearson-R correlation coefficients. These are obtained by applying (2) to the V_P, V_R, V_T, and V_{ST} of the median beats and evaluating the CC on the entire set. Here, the ST segment was defined as the ECG signal in the interval [J+10ms, J+60ms]. The Pearson-R correlation coefficient for the cardiac axis angle (Pearson-R-CA) was evaluated in the same manner as the angles at the P, R, and T points.

TABLE 1. XCORR values for each lead obtained by 4M, EASI, 1M methods.

XCORR	3-lead 4M method	EASI method	1M method
I	0.974	0.965	0.982
II	0.964	0.880	0.957
III	0.897	0.747	0.837
aVR	0.973	0.955	0.975
aVL	0.912	0.558	0.900
aVF	0.939	0.820	0.913
V1	0.966	0.785	0.965
V2	0.975	0.867	0.981
V3	0.976	0.876	0.969
V4	0.964	0.940	0.950
V5	0.966	0.981	0.961
V6	0.968	0.985	0.967
MEAN	0.956	0.863	0.946

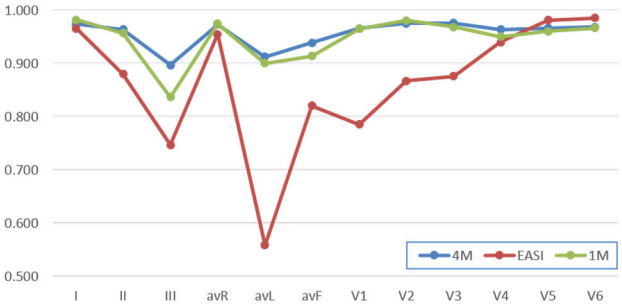

FIGURE 6. The maximal cross-correlation values on all leads for the 4M (blue line), 1M (green line) and EASI method (red line).

TABLE 2. MEANdiff, SDdiff and Pearson-R of the ECG signal amplitude obtained by reconstruction using 4M and EASI matrix methods.

Metric / Amplitude (μV)	MEANdiff	SDdiff	Pearson-R
3-lead 4M			
P wave	-1.37	35.28	0.860
QRS maximum	-27.61	161.93	0.986
T wave	-12.96	73.92	0.958
ST segment	-2.52	34.54	0.779
EASI			
P wave	9.17	55.74	0.706
QRS maximum	187.99	508.80	0.851
T wave	-19.35	125.53	0.873
ST segment	-14.88	26.73	0.840

An additional morphological assessment was performed by comparing the difference in the median-beat amplitudes of V_P, V_R, V_T, and V_{ST} of the tested and reference signals, as well as the difference in the cardiac axis angles at these points. The performance metrics are defined as the mean (MEANdiff for amplitudes and MEANdiff-CA for axis) and standard deviation (SDdiff from amplitudes and SDdiff-CA for axis) of these differences on the whole set.

III. RESULTS AND DISCUSSION

As the 3-lead 4M (3L4M) and EASI methods differ by the electrode number and placement, calibration protocol, and reconstruction method, the comparison below refers to the methods as a whole.

The $XCORR_{3L4M}$ and $XCORR_{EASI}$ values obtained for the test set are presented in Table 1 and Fig. 6, respectively. The error trends of the EASI reconstruction stemming from the EASI electrode placement are in agreement with the reconstruction reported in [15]. 3-lead 4M method reconstructed the 12-lead ECG with $XCORR_{3L4M} > 0.93$ on all leads except III and aVL, achieving higher XCORRs than the EASI method on all leads except the precordial V5 and V6. This exception can be explained by the coincidence of the position of EASI electrode A (Fig. 5b) with the position of the V6 electrode and its vicinity to the V5 electrode of the standard ECG. Similarly, the performances of the two methods were nearly equal for the V4 lead. The precordial leads V1-V3 better coincide with the AIMIGo than the EASI lead geometry, which is reflected in the results. The largest difference between the 4M and EASI method performance is in the aVL lead, whereby the 4M method outperforms EASI by 35%. The relatively poor performance of both methods on the aVL lead can be explained by error propagation from the measured to the derived leads. Finally, the better performance of the 3-lead 4M method is also evidenced by the 96% high mean $XCORR_{3L4M}$ on all leads, which is 10% higher than the mean $XCORR_{EASI}$.

Comparative results for the MEANdiff, SDdiff, and Pearson-R correlation coefficients calculated for the amplitudes of the key segments are given in Table 2. The full statistics are shown in the corresponding Bland-Altman plots in Fig. 7. $MEANdiff_{3L4M}$ and $SDdiff_{3L4M}$ were significantly lower than $MEANdiff_{EASI}$ and $SDdiff_{EASI}$ in all segments except ST. The values of Pearson-R coefficients corroborate this observation, with $Pearson\text{-}R_{3L4M}$ exceeding $Pearson\text{-}R_{EASI}$ by at least 10% in these three segments. The greatest advantage of the 3-lead 4M method was observed in the QRS segment. On the ST segment, the 3-lead 4M method reconstructs the standard ECG with a smaller MEANdiff than the EASI method. However, it shows a comparable yet larger standard deviation (34.5 vs. 26.7) and slightly lower Pearson-R correlation (0.78 vs. 0.84) of amplitudes on the ST segment. The lower performance of the 3-lead 4M method on ST compared to the other segments is due to the nearly isoelectric ST segment in healthy people.

In other words, the near-zero amplitude contains a substantial noise component, which causes scatter of the reconstructed data around zero. Based on the excellent 4M performance on other segments, we expect a more faithful ST-segment reconstruction in the case of acute MI characterized by ST elevation from the isoelectric line.

Metrics for the cardiac axis angle at the P, R, and T points are given in Table 3 and Fig. 8. MEANdiff-CA in the R and T points was almost 10 times lower, and SDdiff-CA was nearly two times lower for 3-lead 4M than for EASI reconstruction. The corresponding Pearson-R coefficients for the 3-lead 4M method exceed those for the EASI method by more than 0.1. Therefore, the 3L4M method reconstructs the QRS complex

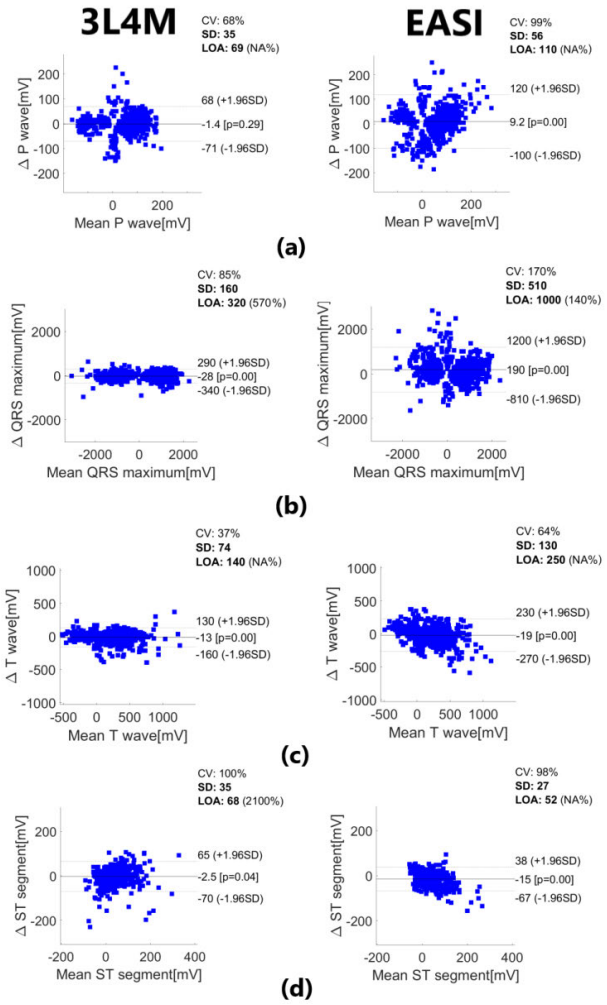

FIGURE 7. Bland-Altman plots of amplitude in: (a) P waves, (b) R waves, (c) T waves, and (d) ST segments obtained from the 3-lead 4M method (left) or EASI method (right) with respect to the reference method. SD – standard deviation, CV – coefficient of variation (SD of mean values in %), LOA – limits of agreement =1.96 SD, and p – p-value for the paired samples t-test.

and T-wave amplitude with more accuracy and precision than the EASI method.

SDdiff-CA and Pearson-R-CA metrics clearly indicate that the cardiac axis angle reconstruction at the P point is challenging for both methods, with a somewhat better performance of the 3-lead 4M method.

The results of the clinical analysis performed by two expert cardiologists are shown in Table 4. The readers agreed that 87.5% of the reconstructions did not differ with respect to the standard ECG. Their reports on the differences agreed in only one recording, which rendered a low kappa coefficient of 0.16 for the binary 'yes'/'no' classification. All differences between the reconstructed and reference signals were minor and would neither interfere with clinical decision-making nor require repeated application of standard ECG for final consolidation. The discrepancies comprised a minor difference in sensitivity for right-sided intraventricular conduction delay

TABLE 3. MEANdiff, SDdiff and Pearson-R of the cardiac axes angle obtained by reconstruction using 4M and EASI matrix methods.

Metric / Angle (deg)	MEANdiff-CA	SDdiff-CA	Pearson-R-CA
3-lead 4M			
P wave	-3.61	37.15	0.236
QRS maximum	-2.39	8.24	0.967
T wave	-0.31	10.24	0.833
EASI			
P wave	6.96	48.32	0.098
QRS maximum	16.65	20.07	0.785
T wave	7.04	26.43	0.713

TABLE 4. Comparison of the 4M-recontructed and standard 12-lead ECG evaluated by expert cardiologist.

Reader	No difference	Diagnostically insignificant difference	Diagnostically significant difference
I	59	5	0
II	60	4	0

detection (with the reconstructed performing better than the standard ECG), attenuation of P waves in some of the leads (not all), change in T-wave voltage direction and amplitude in isolated leads, limited differences in detection and presentation of micro Q waves in specific leads, and in the QRS amplitude and width. The differences between the reconstructed and standard 12-lead ECG were within the variations that may be caused by displacement in electrode positioning for a few centimeters, respiratory variations, or the presence of enhanced vagal tone.

A typical example of a successful 3-lead 4M reconstruction is shown in Fig. 9a. Examples of less-successful reconstructions are shown in Fig. 9b and 9c. Figure 9b shows a failure to reconstruct the P-waves present in the original recording. P-waves are narrow and of low voltage in lead III and most of the precordial leads, while they are attenuated but visible in leads I, II, and aVL. Overall, the diagnostic value for determining baseline driving rhythm was preserved. In addition, the visibility of the P-wave in lead aVL carries correct information on the presence of P-waves, which is highly relevant to the diagnosis of arrhythmias originating in the atria. Figure 9c presents the failure to reconstruct the R-wave spike of the QRS complex in lead III (present as micro R on the original recording) and the full S-wave amplitude in the same lead. Generally, it does not cause a diagnostic dilemma in the presence of a viable myocardium at the inferior wall, because there are positive R waves in the corresponding inferior leads.

Furthermore, we discuss the need for a segment-by-segment approach by comparing the results with 1M reconstruction. The last column in Table 1 shows the XCORR values obtained using the 3-lead 1M method. Both 3-lead 4M and 3-lead 1M methods perform better than the EASI method, except in leads V5 and V6. The reason lies in the position of the AIMIGo electrodes, which more faithfully reproduce standard ECG leads. Electrodes V5 and V6 closely

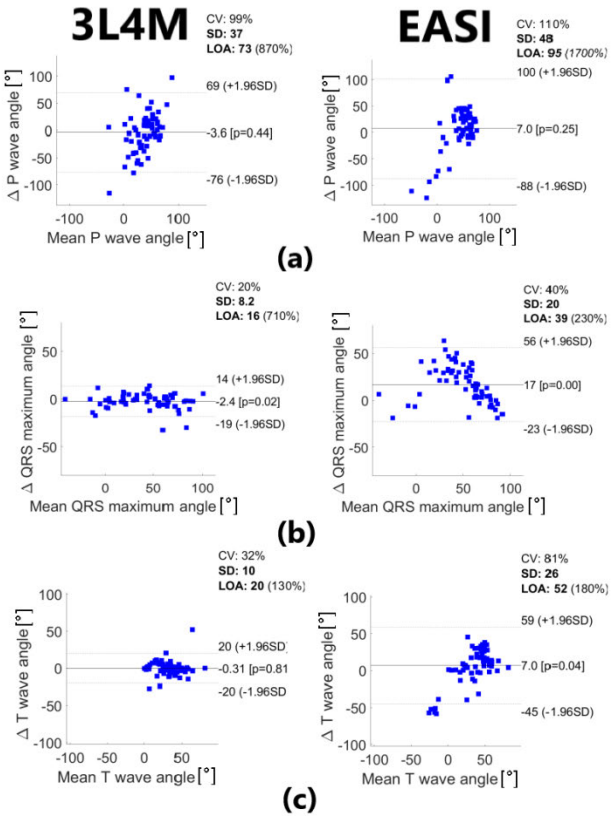

FIGURE 8. Bland-Altman plots of cardiac axis angles in (a) P waves, (b) R waves, and (c) T waves obtained by the 4M method (left) or EASI method (right) with respect to the reference method. SD – standard deviation, CV - coefficient of variation (SD of mean values in %), LOA – limits of agreement =1.96 SD, and p the p-value for the paired samples t-test.

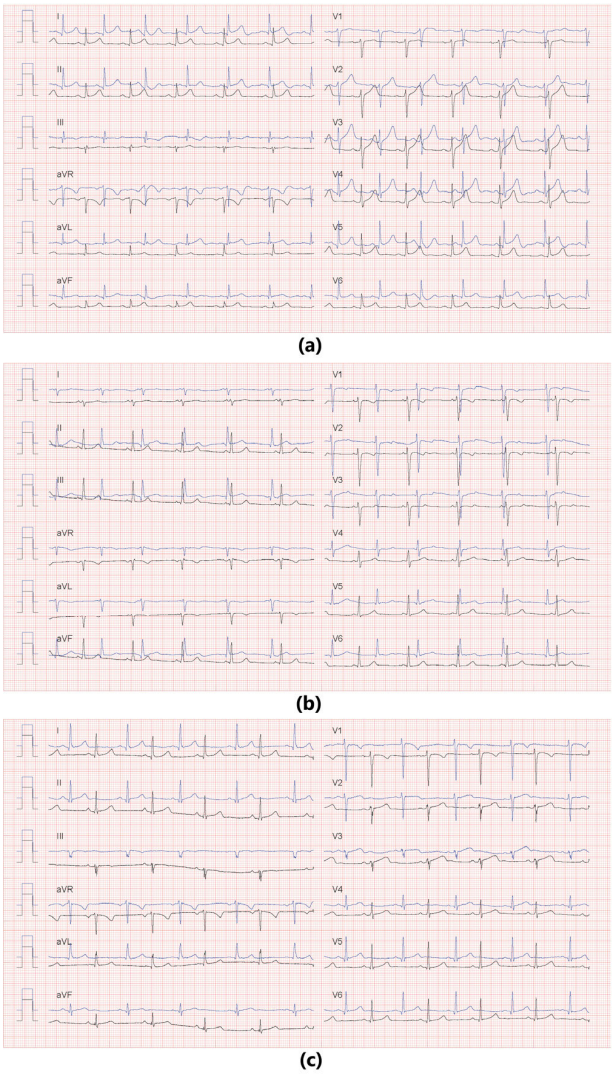

FIGURE 9. Examples of the 12-lead ECG signals reconstructed by 4M method (blue) and the reference signals (black). a) Good agreement with the reference, b) reduced P-wave amplitude in leads II, III, aVF, V1-V6, c) poorly reconstructed the R-wave spike of the QRS complex in lead III.

coincide with EASI electrode A; hence, these leads are better reproduced by the EASI method. The 3-lead 1M method has a lower XCORR score than the 3-lead 4M method in critical leads III, aVL, and aVF with lower-quality reconstruction, while its performance matches that of the 3-lead 4M method for other leads. The difference was most apparent in the Pearson-R coefficients for the cardiac axis angles at the P and T points. The 3-lead 1M method yields 0.158 and 0.495, and the 3-lead 4M method yields 0.236 and 0.833, respectively. Poor reconstruction of the cardiac vector axis by the 3-lead 1M method results in occasional false T-wave inversion, which may cause false alarms for acute MI [34]. The 4M segment-by-segment approach yields 4-times improvement in T-wave reconstruction. Hence, it has the potential to provide cardiologists with more confident decisions on referral to the hospital than both 1M and EASI single-matrix methods. However, diagnostic performance will be the subject of future work.

In this study, the wireless AIMIGo prototype and MATLAB analysis on a PC were used. Calibration was performed for 12 s, and reconstruction was performed for 5 s. We note that the current version of the AIMIGo device is in full wireless operation and is controlled by a software application that communicates with a server on the cloud. Calibration and reconstruction were performed using a cloud server. Reconstruction and 12-lead ECG signal display required approximately 10 s.

IV. CONCLUSION

We addressed the problem of reconstructing the standard 12-lead ECG from an ECG recorded by a mobile 3-lead (3 L) device, which is of high significance for timely self-detection of acute coronary conditions. The proposed 4M reconstruction algorithm is based on matrix multiplication performed segment-by-segment on the P wave, QRS complex, ST interval, and T wave of each beat. The calibration of transfer matrices does not require the simultaneous recording of 3- and 12-lead calibration signals. A study on 64 healthy volunteers showed that the proposed 3-lead 4M method

reconstructs the 12-lead ECG and cardiac vector axis with higher fidelity than the EASI method in all ECG signals except the low-amplitude ST segment. We expect this limitation to be less pronounced in acute MI patients with ST elevation. Moreover, unlike the general/population matrix reconstruction approach, the proposed method contains information about the individual characteristics of each patient, which is known to reduce reconstruction errors.

The presented results prove that a simple self-measurement using a 3-lead handheld device can provide comprehensive information on the 3D cardiac vector, thus setting a milestone in the development of mobile ECG technology. The main challenge is the validation of the 3-lead 4M method in subjects with various diagnoses of clinical importance. The primary target is the diagnosis of acute MI, which has been shown to be possible by vectorcardiographic ST segment analysis [20], but has not been demonstrated by mobile ECG technology.

The full wireless operation of AIMIGo and the 5-s reconstruction make the device suitable for mobile self-evaluation.

The 4M algorithm, which includes calibration and reconstruction used in the measurement study, is implemented on the cloud. The main limitation in the clinical application of the entire system is the requirement for high-speed internet, which is needed for uninterrupted data transfer between the measurement software on the smartphone and the cloud server and for displaying the ECG signal in a web browser on a doctor's PC following measurement and reconstruction. The execution speed of the calibration and reconstruction algorithms could be improved by implementing the algorithms in programming languages that offer faster execution than MATLAB, such as C++ or C#.

V. LIMITATIONS OF THE STUDY

The main limitations of this study were the relatively small set size of 64 volunteers and the fact that all subjects were healthy and white. To overcome these limitations, we are currently conducting two clinical studies, which will assess the performance of the 3-lead 4M method in patients with various arrhythmias and ischemia provoked by percutaneous coronary intervention. The recruited patient cohorts are significantly larger and compliant with the diversity criteria.

APPENDIX A

The heart vector at the k^{th} time point is defined as the root sum square of the leads of a 3-lead ECG (Xi, i=1,2,3) at a certain time point and is given by

$$P_k = \sqrt{X_{1,k}^2 + X_{2,k}^2 + X_{3,k}^2} \tag{3}$$

where k is k^{th} time sample (point).

CONFLICT OF INTEREST

3-lead AIMIGo measurement and 4M reconstruction method are covered by the US10117592B2 [28] and US11445963B1 [35] patents assigned to the company HeartBeam Inc., Santa Clara, CA, USA.

Marjan N. Miletić, Vladimir A. Atanasoski, Petra P. Beličev, Goran M. Gligorić, Danka B. Stojanović, Jelena B. Kršić, Uroš M. Ralević, Jovana Petrović, Ljupčo R. Hadžievski, Boško P. Bojović, and Branislav Vajdić are with HeartBeam Inc.

REFERENCES

[1] A. Timmis, "European society of cardiology: Cardiovascular disease statistics 2017," *Eur. Heart J.*, vol. 39, pp. 508–579, Jun. 2017.

[2] A. Bhatia and T. M. Maddox, "Remote patient monitoring in heart failure: Factors for clinical efficacy," *Int. J. Heart Failure*, vol. 3, no. 1, pp. 31–50, 2021.

[3] N. M. de Vries, A. Zepeda-Echavarria, R. R. van de Leur, V. Loen, M. A. Vos, M. J. Boonstra, T. X. Wildbergh, J. E. N. Jaspers, R. van der Zee, C. H. Slump, P. A. Doevendans, and R. van Es, "Detection of ischemic ST-segment changes using a novel handheld ECG device in a porcine model," *JACC: Adv.*, vol. 2, no. 5, Jul. 2023, Art. no. 100410.

[4] A. Bansal and R. Joshi, "Portable out-of-hospital electrocardiography: A review of current technologies," *J. Arrhythmia*, vol. 34, no. 2, pp. 129–138, Apr. 2018.

[5] J. Malmivuo and R. Plonsey, "12-lead ECG system," in *Bioelectromagnetism*, vol. 15. London, U.K.: Oxford Univ. Press, 1995.

[6] M. P. Donnelly, D. D. Finlay, C. D. Nugent, and N. D. Black, "Lead selection: Old and new methods for locating the most electrocardiogram information," *J. Electrocardiology*, vol. 41, no. 3, pp. 257–263, May 2008.

[7] H. Yang, S. T. Bukkapatnam, and R. Komanduri, "Spatiotemporal representation of cardiac vectorcardiogram (VCG) signals," *Biomed. Eng. OnLine*, vol. 11, no. 1, p. 16, 2012.

[8] I. Tomašic and R. Trobec, "Electrocardiographic systems with reduced numbers of leads—Synthesis of the 12-lead ECG," *IEEE Rev. Biomed. Eng.*, vol. 7, pp. 126–142, 2014.

[9] G. E. Dower, A. Yakush, S. B. Nazzal, R. V. Jutzy, and C. E. Ruiz, "Deriving the 12-lead electrocardiogram from four (EASI) electrodes," *J. Electrocardiology*, vol. 21, pp. S182–S187, Jan. 1988.

[10] B. J. Drew, M. M. Pelter, S.-F. Wung, M. G. Adams, C. Taylor, G. T. Evans, and E. Foster, "Accuracy of the EASI 12-lead electrocardiogram compared to the standard 12-lead electrocardiogram for diagnosing multiple cardiac abnormalities," *J. Electrocardiology*, vol. 32, pp. 38–47, Jan. 1999.

[11] P. M. Rautaharju, S. H. Zhou, E. W. Hancock, D. Q. Feild, J. M. Lindauer, G. S. Wagner, O. Pahlm, and C. L. Feldman, "Comparability of 12-lead ECGs derived from EASI leads with standard 12-lead ECGS in the classification of acute myocardial ischemia and old myocardial infarction," *J. Electrocardiology*, vol. 35, no. 4, pp. 35–39, Oct. 2002.

[12] G. Wehr, R. J. Peters, K. Khalifé, A. P. Banning, V. Kuehlkamp, A. F. Rickards, and U. Sechtem, "A vector-based, 5-electrode, 12-lead monitoring ECG (EASI) is equivalent to conventional 12-lead ECG for diagnosis of acute coronary syndromes," *J. Electrocardiology*, vol. 39, no. 1, pp. 22–28, Jan. 2006.

[13] D. Chantad, R. Krittayaphong, and C. Komoltri, "Derived 12-lead electrocardiogram in the assessment of ST-segment deviation and cardiac rhythm," *J. Electrocardiology*, vol. 39, no. 1, pp. 7–12, Jan. 2006.

[14] B. J. Drew, M. G. Adams, M. M. Pelter, S.-F. Wung, and M. A. Caldwell, "Comparison of standard and derived 12-lead electrocardiograms for diagnosis of coronary angioplasty-induced myocardial ischemia," *Amer. J. Cardiology*, vol. 79, no. 5, pp. 639–644, Mar. 1997.

[15] D. Q. Feild, C. L. Feldman, and B. M. Horacek, "Improved EASI coefficients: Their derivation, values, and performance," *J. Electrocardiology*, vol. 35, no. 4, pp. 23–33, Oct. 2002.

[16] B. Redfors, "Time delay, infarct size, and microvascular obstruction after primary percutaneous coronary intervention for ST-segment-elevation myocardial infarction," *Circ. Cardiovasc. Interv.*, vol. 14, p. 2, Feb. 2021.

[17] E. Svennberg, "How to use digital devices to detect and manage arrhythmias: An EHRA practical guide," *EP Europace*, vol. 24, no. 6, pp. 979–1005, Jul. 2022.

[18] J. B. Muhlestein, V. Le, D. Albert, F. L. Moreno, J. L. Anderson, F. Yanowitz, R. B. Vranian, G. W. Barsness, C. F. Bethea, H. W. Severance, B. Ramo, J. Pierce, A. Barbagelata, and J. B. Muhlestein, "Smartphone ECG for evaluation of STEMI: Results of the ST LEUIS pilot study," *J. Electrocardiology*, vol. 48, no. 2, pp. 249–259, Mar. 2015.

[19] M. P. Witvliet, E. P. M. Karregat, J. C. L. Himmelreich, J. S. S. G. de Jong, W. A. M. Lucassen, and R. E. Harskamp, "Usefulness, pitfalls and interpretation of handheld single'lead electrocardiograms," *J. Electrocardiology*, vol. 66, pp. 33–37, May 2021.
[20] A. Shvilkin, D. Vukajlović, B. P. Bojović, L. R. Hadžievski, B. Vajdic, V. A. Atanasoski, M. N. Miletić, P. J. Zimetbaum, C. M. Gibson, and V. Vukčević, "Coronary artery occlusion detection using 3-lead ECG system suitable for credit card-size personal device integration," *JACC, Adv.*, vol. 2, no. 6, Aug. 2023, Art. no. 100454.
[21] A. Behzadi, A. S. Shamloo, K. Mouratis, G. Hindricks, A. Arya, and A. Bollmann, "Feasibility and reliability of SmartWatch to obtain 3-lead electrocardiogram recordings," *Sensors*, vol. 20, no. 18, p. 5074, Sep. 2020.
[22] A. Aranda, P. Bonizzi, J. Karel, and R. Peeters, "Performance of Dower's inverse transform and Frank lead system for identification of myocardial infarction," in *Proc. Conf. IEEE Eng. Med. Biol. Soc.*, 2015, pp. 4495–4498.
[23] M. El Haddad, D. Vervloet, Y. Taeymans, M. De Buyzere, T. Bové, R. Stroobandt, M. Duytschaever, J. Malmivuo, and P. Gheeraert, "Diagnostic accuracy of a novel method for detection of acute transmural myocardial ischemia based upon a self-applicable 3-lead configuration," *J. Electrocardiology*, vol. 49, no. 2, pp. 192–201, Mar. 2016.
[24] A. Zepeda-Echavarria, R. R. van de Leur, M. Vessies, N. M. de Vries, M. van Sleuwen, R. J. Hassink, T. X. Wildbergh, J. L. van Doorn, R. van der Zee, P. A. Doevendans, J. E. N. Jaspers, and R. van Es, "Detection of acute coronary occlusion with a novel mobile electrocardiogram device: A pilot study," *Eur. Heart J. Digit. Health*, vol. 5, no. 2, pp. 183–191, Mar. 2024.
[25] L. Hadzievski, B. Bojovic, V. Vukcevic, P. Belicev, S. Pavlovic, Z. Vasiljevic-Pokrajcic, and M. Ostojic, "A novel mobile transtelephonic system with synthesized 12-lead ECG," *IEEE Trans. Inf. Technol. Biomed.*, vol. 8, no. 4, pp. 428–438, Dec. 2004.
[26] V. Atanasoski, J. Petrovic, L. P. Maneski, M. Miletić, M. Babić, A. Nikolić, D. Panescu, and M. D. Ivanović, "A morphology-preserving algorithm for denoising of EMG-contaminated ECG signals," *IEEE Open J. Eng. Med. Biol.*, vol. 5, pp. 296–305, 2024.
[27] Heart Beam Inc. (2024). *HeartBeam is Developing a Personal, Portable, and Easy-to-Use System for Cardiac Monitoring*. [Online]. Available: https://www.heartbeam.com
[28] B. Bojovic, L. Hadzievski, V. Vukcević, U. Mitrović, and M. Miletić, "Mobile three-lead cardiac monitoring device and method for automated diagnostics," U.S. Patent 10 117 592 B2, Nov. 6, 2017.
[29] G. S. Wagner, P. Macfarlane, H. Wellens, M. Josephson, A. Gorgels, D. M. Mirvis, O. Pahlm, B. Surawicz, P. Kligfield, R. Childers, and L. S. Gettes , "AHA/ACCF/HRS recommendations for the standardization and interpretation of the electrocardiogram: Part VI: Acute ischemia/infarction: A scientific statement from the American Heart Association electrocardiography and arrhythmias committee, council on clinical cardiology; the American college of cardiology foundation; and the heart rhythm society: Endorsed by the international society for computerized electrocardiology," *Circulation*, vol. 119, no. 10, pp. 262–270, Mar. 2009.
[30] E. W. Hancock, B. J. Deal, D. M. Mirvis, P. Okin, P. Kligfield, and L. S. Gettes, "AHA/ACCF/HRS recommendations for the standardization and interpretation of the electrocardiogram: Part V: Electrocardiogram changes associated with cardiac chamber hypertrophy: A scientific statement from the American Heart Association electrocardiography and arrhythmias committee, council on clinical cardiology; the American college of cardiology foundation; and the heart rhythm society," *Circulation*, vol. 119, no. 10, pp. 251–261, Mar. 2009.
[31] P. M. Rautaharju, B. Surawicz, and L. S. Gettes, "AHA/ACCF/HRS recommendations for the standardization and interpretation of the electrocardiogram: Part IV: The ST segment, t and u waves, and the QT interval: A scientific statement from the American Heart Association electrocardiography and arrhythmias committee, council on clinical cardiology; the American college of cardiology foundation; and the heart rhythm society: Endorsed by the international society for computerized electrocardiology," *Circulation*, vol. 119, no. 10, pp. 241–250, Mar. 2009.
[32] B. Surawicz, R. Childers, B. J. Deal, and L. S. Gettes, "AHA/ACCF/HRS recommendations for the standardization and interpretation of the electrocardiogram: Part III: Intraventricular conduction disturbances: A scientific statement from the American Heart Association electrocardiography and arrhythmias committee, council on clinical cardiology; the American college of cardiology foundation; and the heart rhythm society," *Circulation*, vol. 119, no. 10, pp. 976–981, Mar. 2009.
[33] J. W. Mason, E. W. Hancock, and L. S. Gettes, "Recommendations for the standardization and interpretation of the electrocardiogram. Part II: Electrocardiography diagnostic statement list: A scientific statement from the American Heart Association electrocardiography and arrhythmias committee, council on clinical cardiology; the American college of cardiology foundation; and the heart rhythm society. Endorsed by the international society," *Hear. Rhythm*, vol. 4, pp. 413–419, Jun. 2007.
[34] A. L. Goldberger, "Deep T wave Inversions. Myocardial ischemia and infarction, part II," in *Goldberger's Clinical Electrocardiography*, 9th ed. Amsterdam, The Netherlands: Elsevier, 2018.
[35] P. Belicev, B. Bojovic, L. Hadzievski, B. Vajdic, V. Atanasoski, G. Gligoric, and M. Miletic, "Method and apparatus for reconstructing electrocardiogram (ECG) data," US Patent 11 445 963 B1, Sep. 20, 2022.

MARJAN N. MILETIĆ received the B.S. degree in electrical engineering from the School of Electrical Engineering, University of Belgrade, Belgrade, Serbia, where he is currently pursuing the Ph.D. degree in biomedical engineering and technologies.

He was a Research Assistant (2015–2022) and a Principal Technical Associate (since 2022) with the Vinča Institute of Nuclear Sciences–National Institute of the Republic of Serbia, University of Belgrade. His research interests include biomedical signal analysis, data processing, and machine learning.

VLADIMIR A. ATANASOSKI is currently pursuing the Ph.D. degree in biomedical engineering with the University of Belgrade, Serbia. He has been a Technical Associate with the Vinča Institute of Nuclear Sciences, University of Belgrade, since 2022. Since 2016, he has been a Research and Development Engineer with HeartBeam Inc. His research interests include biomedical signal processing and machine learning.

PETRA P. BELIČEV received the Ph.D. degree in electrical engineering from the School of Electrical Engineering, University of Belgrade, Belgrade, Serbia, in 2012. She is a Research Associate Professor with the Vinča Institute of Nuclear Sciences, University of Belgrade. She has 15 years of research experience in photonics. Since 2015, her research interests have been expanded to biomedical signal analysis and the development of medical diagnostic devices.

GORAN M. GLIGORIĆ received the Ph.D. degree in electrical engineering from the School of Electrical Engineering, University of Belgrade, Serbia, in 2010. His research interests include the field of physics of complex systems, nonlinear optics, and signal processing.

UROŠ M. RALEVIĆ received the Ph.D. degree in electrical engineering from the School of Electrical Engineering, University of Belgrade, Serbia, in 2017. His research interests include the field of physics of low dimensional systems, plasmonics, and signal processing.

JELENA B. KRŠIĆ received the master's degree in physics from the Faculty of Physics, University of Belgrade, Belgrade, Serbia. She is currently pursuing the Ph.D. degree in physics with the University of Nis, Serbia.

She was a Research Trainee (2016–2021) and a Senior Technical Associate (since 2021) with the Vinča Institute for Nuclear Sciences–National Institute of the Republic of Serbia, University of Belgrade. Her research interests include the fields of biophysics and optics.

ALEKSA D. OBRADOVIĆ, photograph and biography not available at the time of publication.

ALEKSANDAR LAZOVIĆ, photograph and biography not available at the time of publication.

DANKA B. STOJANOVIĆ, photograph and biography not available at the time of publication.

JOVANA PETROVIĆ, photograph and biography not available at the time of publication.

RADE BABIĆ received the M.D. and Ph.D. degrees. He completed a Postdoctoral degree in interventional cardiology from Milan, Italy, and in cardiac electrophysiology from Ashkelon, Israel.

He is a Full Professor of internal medicine/cardiology with the University of Belgrade. Previously, he was with the Institute for Cardiovascular Diseases, Clinical Centre of Serbia, Belgrade; and the Cardiovascular Institute "Dedinje," Belgrade. Currently, he is a Consultant with the University Hospital Centre Dr. Dragisa Misovic, Belgrade. His research interests include coronary heart disease, interventional cardiology, heart failure, cardiac arrhythmias, and image processing in cardiology. He is a fellow of FESC and FSCAI.

DEJAN VUKAJLOVIĆ, photograph and biography not available at the time of publication.

LJUPČO R. HADŽIEVSKI, photograph and biography not available at the time of publication.

BOŠKO P. BOJOVIĆ, photograph and biography not available at the time of publication.

DORIN PANESCU, photograph and biography not available at the time of publication.

BRANISLAV VAJDIĆ, photograph and biography not available at the time of publication.